Resistance and current-voltage characteristics of individual superconducting $NbSe_2$ nanowires

Zhixian Zhou,[1,*] Rongying Jin,[1] Gyula Eres,[1] David Mandrus,[1] Victor Barzykin,[2] Pedro Schlottmann,[3] Yew-San Hor,[4] Zhili Xiao,[4,5] and John F. Mitchell[4]

[1]*Materials Science and Technology Division, Oak Ridge National Laboratory, Oak Ridge, Tennessee 37831, USA*
[2]*Department of Physics and Astronomy, University of Tennessee, Knoxville, Tennessee 37996, USA*
[3]*Department of Physics, Florida State University, Tallahassee, Florida 32306, USA*
[4]*Materials Science Division, Argonne National Laboratory, Argonne, Illinois 60439, USA*
[5]*Department of Physics, Northern Illinois University, DeKalb, Illinois 60115, USA*

(Received 25 May 2007; revised manuscript received 30 July 2007; published 18 September 2007)

Resistance and current-voltage characteristics of individual superconducting $NbSe_2$ nanowires are investigated. In the current-voltage curves, a stairlike structure is observed, indicating the possible formation of phase-slip centers. A close examination of the current-voltage characteristic in a selected high quality $NbSe_2$ nanowire with a diameter of 75 nm reveals that the characteristic voltages in the stairlike structure follow the BCS-like temperature dependence of superconducting gaps vanishing at T_C. While the phase-slip center mechanism remains to be a plausible explanation of the observed features, an alternative model involving multigap Josephson tunneling is proposed to account for the BCS-like temperature dependence. From the BCS fits, two distinct superconducting gaps are extracted. Moreover, the critical current of the 75 nm nanowire at low temperatures as well as near T_C can also be described by the Ambegaokar-Baratoff relation for multigap Josephson junctions. Our data suggest the possible observation of multiband superconductivity in $NbSe_2$ and are in good agreement with the predictions of recent band structure and Fermi surface calculations on $NbSe_2$.

DOI: 10.1103/PhysRevB.76.104511 PACS number(s): 74.50.+r, 73.63.−b, 74.25.Jb, 74.25.Sv

I. INTRODUCTION

The existence of distinct superconducting energy gaps on different sheets of the Fermi surface (FS) gives rise to an unusual phenomenon termed as multiband superconductivity (MBSC). The observation of this phenomenon in MgB_2, a phonon-mediated *s*-wave superconductor with a high transition temperature, T_C=39 K, has spurred considerable research interest in the physics of MBSC.[1–3] To gain a deeper understanding of the physics of MBSC, it is important to study multiband superconductors other than MgB_2. $NbSe_2$ is another system that is host to MBSC. $NbSe_2$ as a classic type-II superconductor has been studied intensively over the past four decades. A variety of interesting phenomena have been discovered in this system, including the coexistence of seemingly competitive charge density wave (CDW) order and superconductivity and the "peak effect."[4–6] An early study on the superconducting gap of $NbSe_2$ using far-infrared transmission spectroscopy has shown that the temperature dependence of the gap energy is in good agreement with the BCS theory over the limited temperature range of measurement.[7] Johannes *et al.* have demonstrated in their recent density function calculations that the FS sheets of $NbSe_2$ can be divided into two groups: the small Se-derived pancake surface around the Γ point and the large bonding and antibonding Nb-derived FS sheets.[4] In addition, they predicted that these two sets of FS sheets with different gap sizes can be probed by tunneling measurements. Experimentally, however, the low temperature scanning tunneling spectroscopy measurements performed on $NbSe_2$ single crystals only indicated a distribution of energy gaps between 0.6 and 1.3 meV.[8] Angle resolved photoemission spectroscopy measurements revealed a sizable difference in the magnitude of the superconducting gap on two sets of FS sheets at 5.3 K only.[9]

The superconducting $NbSe_2$ nanowires (NWs) recently synthesized by Hor *et al.* provide a new platform for studying the MGSC in $NbSe_2$, and the observation of grain boundaries (GBs) in some of the NWs by transmission electron microscopy (TEM) inspired us to study the MGSC in $NbSe_2$ through GB tunneling.[10] These NWs are also good candidates for studying the current-induced breakdown of superconductivity, which has been a long-standing problem of recurrent interest.[11–13] As the bias current is raised above a local minimum critical current of a NW, a phase-slip center (PSC) develops, creating a finite voltage. The successive nucleation of PSCs leads to the appearance of a stairlike structure in the *I-V* characteristics.[13]

In this paper we report electrical transport studies of individual $NbSe_2$ NWs. A stairlike structure has been observed in the current-voltage (*I-V*) characteristic, indicating the possible formation of PSCs under a bias current. The temperature dependences of the characteristic voltages in the *I-V* characteristic of a selected $NbSe_2$ NW with a diameter of 75 nm follow the BCS-like temperature dependence of superconducting gaps. Accordingly, an alternative mechanism involving the multigap Josephson tunneling is proposed to explain the observed BCS-like temperature dependences, which cannot be understood in the context of phase slips. The extrapolated superconducting gaps are in quantitative agreement with the theory.[4] We have also found that the critical current of the 75 nm diameter $NbSe_2$ NW is consistent with the theoretical predictions of Ambegaokar and Baratoff.[14]

II. EXPERIMENTAL DETAILS

$NbSe_2$ NWs were synthesized from $NbSe_3$ NWs and Nb powder.[10] The as-grown NWs have the crystal structure of

$2H$-$NbSe_2$ as determined by x-ray diffraction. Although nearly perfect electron diffraction patterns were observed in selected areas, grain boundaries were indeed found inside some NWs through high-resolution TEM imagining.[10] In order to perform electrical transport measurements on individual $NbSe_2$ NWs, they were first ultrasonically dispersed in isopropyl alcohol, and then deposited onto Si/SiO_2 substrates with predefined alignment marks. Subsequently, custom metal electrodes were defined by electron beam lithography followed by electron-gun assisted deposition of a 10 nm Ti adhesion layer and 200 nm of Au. Fast thermal annealing at 400 °C was carried out in vacuum (10^{-7} torr) to improve the electrical contacts. Both four-probe (4P) and two-probe devices were fabricated. Electrical transport measurements were carried out in a Quantum Design physical properties measurement system.

III. RESULTS AND DISCUSSIONS

We have fabricated and characterized over 40 devices, most of which showed signatures of impurity phases such as the two CDW transitions of $NbSe_3$.[15] High quality devices are obtained only in optimally converted NWs. In this paper, we focus on one 4P device with high sample quality. For comparison, data on a slightly underconverted $NbSe_2$ NW (but without the signatures of $NbSe_3$) and two other high quality $NbSe_2$ NWs of substantially larger diameters are also presented and briefly discussed. Figure 1 shows the low bias ($I=200$ nA$\ll I_C$) resistance R as a function of temperature T for the 4P device consisting of a 75 nm diameter superconducting $NbSe_2$ NW as depicted in the lower right inset of Fig. 1(b). The general aspects of the $R(T)$ data resemble those of $NbSe_2$ bulk crystals, except that the T_C in this NW is suppressed from the typical bulk value of 7.2 K to 6.6 K.[16] The slight decrease of T_C may be attributed to the polycrystalline nature of the wire.[17,18] In the normal state, a hump is seen in $R(T)$ [Fig. 1(b)], corresponding to the CDW transition of $NbSe_2$ with $T_{CDW}=33$ K determined by plotting dR/T as a function of T, indicating high sample quality.[16,19,20]

Figure 2(a) shows the voltage-current (V-I) characteristics of the NW for $T<T_C$, applying a gradually increasing dc current. The voltage drop is immeasurably low at low bias currents until the critical current I_C is reached, where the voltage jumps abruptly from zero to a finite value before entering a dissipative region with a linear V-I at higher bias currents. Nearly identical results were obtained with reversed polarity, while the V-I characteristic was always measured with increasing I. At low temperatures, a stairlike structure is clearly visible within the big voltage jump, which in superconducting NWs is often attributed to the formation of PSCs.[11–13]

Since the self-field generated by the current does not exceed the lower critical field in the wire (or at the surface), we rule out the possibility of filamentary vortex flow, which may also generate steps in V-I curves.[21–24] In Fig. 2(b), we plot the T dependence of the critical current I_C (defined as the maximum supercurrent). For $0.85T_C<T<T_C$, I_C increases linearly with decreasing T, significantly deviating from the Ginzburg-Landau theory, which predicts $I_C\sim(1-T/T_C)^{3/2}$

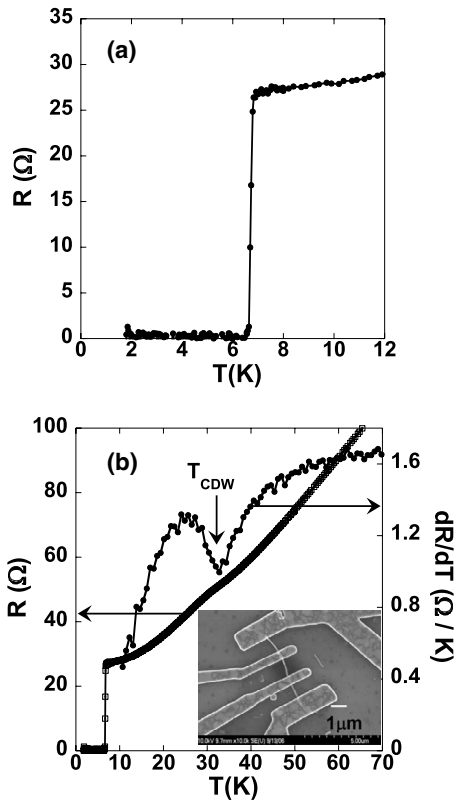

FIG. 1. (a) Resistance versus temperature for a superconducting $NbSe_2$ NW with a diameter of ~75 nm, applying a current of 200 nA. (b) R and dR/dT versus T of the $NbSe_2$ NW device for a broader temperature range. Inset: A SEM image of the $NbSe_2$ NW device.

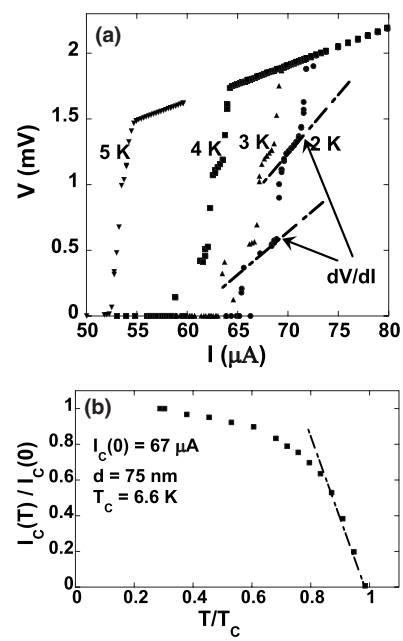

FIG. 2. (a) Voltage-current (V-I) curves of the 4P $NbSe_2$ NW device measured in zero applied magnetic field for $T<T_C$. (b) Temperature dependence of the reduced critical current.

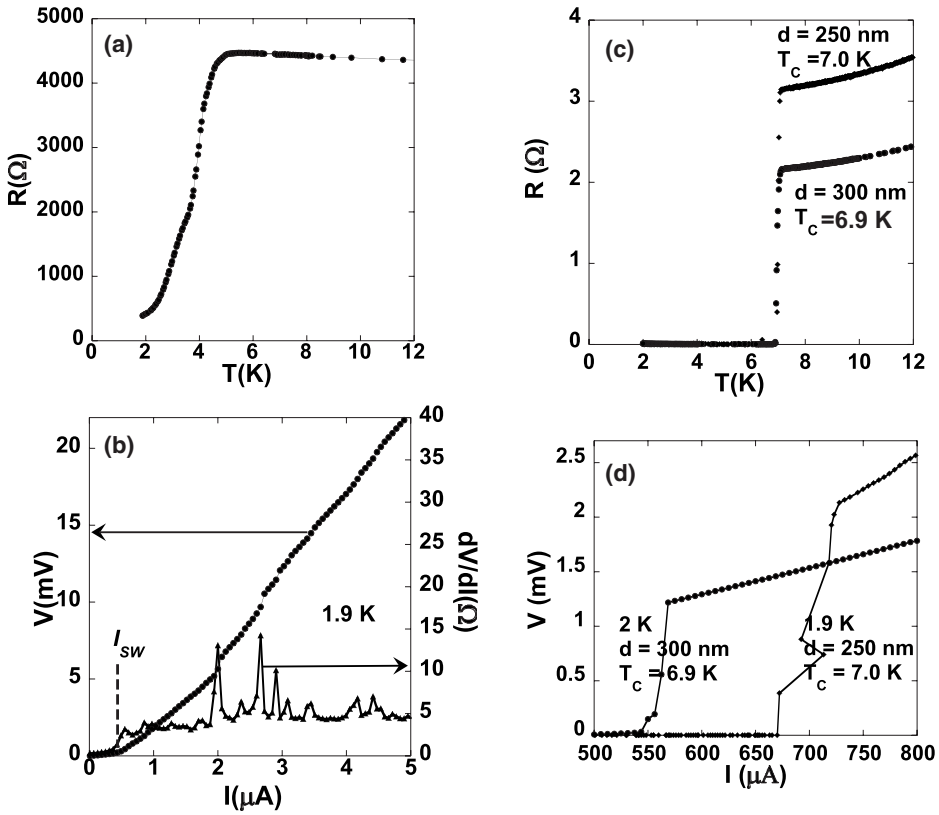

FIG. 3. (a) Resistance versus temperature for an underconverted superconducting $NbSe_2$ NW with a diameter of ~40 nm, applying a current of 10 nA. (b) Voltage-current (*V-I*) curves and dV/dI of the $NbSe_2$ NW device in (a) measured in zero applied magnetic field at $T=1.9$ K. (c) R versus T for two high quality $NbSe_2$ NWs with diameters of 250 and 300 nm, respectively. (d) Voltage-current (*V-I*) curves of the two $NbSe_2$ NW devices in (c); the 250 and 300 nm NWs are measured in zero applied magnetic field and at 1.9 and 2 K, respectively.

near T_C. This discrepancy casts reasonable doubt on "pair breaking" (at a critical velocity of the Cooper pairs) as a possible current-limiting mechanism in our NW.[25–27]

Falk *et al.* also observed stairlike structures in their $NbSe_2$ NWs of comparable or larger diameters but with significantly lower T_C (2–2.3 K), where the voltage steps were attributed to the formation of PSCs possibly due to some type of internal structures arising from the variation of the order parameter over the cross section of the superconductor.[28] Besides the difference in T_C, two other import dissimilarities between our 75 nm $NbSe_2$ NW and their $NbSe_2$ NWs are also noted. First, the voltage drop in our sample is zero at low bias in contrast to the finite V drop in their samples, indicating that thermally activated phase slips (TAPSs) near T_C (Refs. 29–31) and quantum phase slips (QPSs) [13,32–34] which may have contributed to the finite resistances in their samples have a much weaker effect in our NW. Second, the critical current density in our NW is also substantially higher. These differences signify higher sample quality of our selected NW. Although the QPSs and TAPSs are negligible in our sample, the stairlike structure observed in our high quality NW is consistent with the formation of PSCs in thin superconducting filaments such as whisker crystals, thin-film microbridges, and NWs as described by a model proposed by Skocpol, Beasley, and Tinkham (SBT).[11–13] Based on the SBT model, every step in the *V-I* characteristic is associated with the formation of a new PSC with finite resistance. The spatial extent of the PSC is given by the quasiparticle diffusion length $\Lambda = V_{PSC}L/2R_N(I-I_s)$, where V_{PSC} is the voltage contributed by a PSC, L is the length of the sample, and R_N is the normal state resistance. Fitting the L, V_{PSC}, R_N, and $(I-I_s)$ values obtained from Figs. 1 and 2 to the formula, the quasiparticle diffusion length of the 75 nm $NbSe_2$ NW is estimated to be $\Lambda \sim 1$ μm, comparable to L.

For comparison, we have also investigated slightly underconverted $NbSe_2$ NWs (with Se impurities) and high quality $NbSe_2$ NWs with large diameters. Figure 3(a) shows the low bias ($I=10$ nA) $R(T)$ data for a representative slightly underconverted $NbSe_2$ NW device with $d \sim 40$ nm, where not only the onset of T_C is significantly reduced but also the superconducting transition is much broader than that in the high quality sample as depicted in Fig. 1. In addition, the $R(T)$ exhibits two distinct regimes below T_C, similar to the findings of Tian *et al.* in their Sn NWs, where the $R(T)$ data were interpreted as a superposition of TAPS near T_C and QPS far below T_C.[35] Although the relatively small diameter (~40 nm) of the underconverted $NbSe_2$ NW may contribute to the TAPS and QPS, similar phenomena such as significantly reduced T_C and a resistance tail have also been observed in our underconverted $NbSe_2$ NWs with diameters larger than 100 nm. Therefore, as reported by Falk *et al.*, internal structures within the NWs are likely to be the primary cause of the TAPS and QPS in our underconverted $NbSe_2$ NWs. Figure 3(b) shows the *V-I* characteristic and

dV/dI of the same sample as in Fig. 3(a). At very low I, the voltage drop across the NW is small. As I increases above a switching current (I_{SW}), the slope (dV/dI) swiftly increases followed by multiple small voltage steps, which are clearly revealed as peaks in the dV/dI versus I plot. These small voltage steps are also consistent with the PSC scenario. Figures 3(c) and 3(d) show the $R(T)$ and V-I data on two larger diameter $NbSe_2$ NWs, respectively. Sharp superconducting transitions ($\Delta T \approx 0.1$ K) have been observed at temperatures very close to the bulk T_C of $NbSe_2$ (7.0 and 6.9 K for the 250 and 300 nm NWs, respectively). In the V-I characteristic, an abrupt voltage jump from zero to a finite value appears in both samples at I_C. However, we were unable to resolve any internal structures in the large voltage jump at low temperatures, and smaller bias current steps in the transition region only yield increased fluctuations. The absence of voltage steps in the larger diameter samples at low T may be attributed to the heating effect at high power levels.[11]

Based on the low temperature critical currents and the NW diameters determined by scanning electron microscopy (SEM), the critical current densities of the $NbSe_2$ NWs are estimated, yielding comparable values for the three high quality NWs (1.5×10^6 A cm^{-2} for the 75 nm, 1.4×10^6 A cm^{-2} for the 250 nm, and 7.8×10^5 A cm^{-2} for the 300 nm samples) and a much lower critical current density for the slightly underconverted NW (1.6×10^5 A cm^{-2}), where the I_C in the underconverted NW is defined as the current at which the first jump in the V-I occurs. The critical current densities of our $NbSe_2$ NWs are consistent with the current-induced phase-slip scenario, in which the nucleation of PSC occurs at the same critical current density for NWs with similar material characteristics.[13] The substantially lower critical current density of the underconverted NW can be attributed to its smaller diffusion constant D.[11] Even in the high quality samples, the critical current density is still substantially below the critical depairing current density, possibly due to the voltage driven nonequilibrium of the quasiparticles.[36] Since $\Lambda \propto \sqrt{D}$, the quasiparticle diffusion length of the underconverted $NbSe_2$ NW is also smaller, which may contribute to the larger number of voltage steps observed in its V-I characteristic. Within the framework of the SBT model, the differential resistance of the linear V-I region following each voltage jump $dV/dI \approx 2\Lambda\rho/A$, where ρ and A are the resistivity and cross section of the sample, respectively.[11] Therefore, the differential resistance associated with each PSC is expected to be smaller than the total normal state resistance. However, the differential resistances associated with the two voltage steps in our 75 nm NW are both significantly larger than the total normal resistance of the sample [see Fig. 2(a)]. We do not understand this discrepancy, but speculate that it may be caused by the interactions between the PSCs and the electrodes.

To shed more light on the origin of the stairlike structure (which may be connected to the current-limiting mechanism), a close examination of the I-V characteristic in the finite voltage region is necessary. In Fig. 4(a), we replot the data shown in Fig. 2(a) in the form of current versus voltage (I-V). The sudden increase of the voltage at the critical current and the subsequent entrance to the linear I-V region is

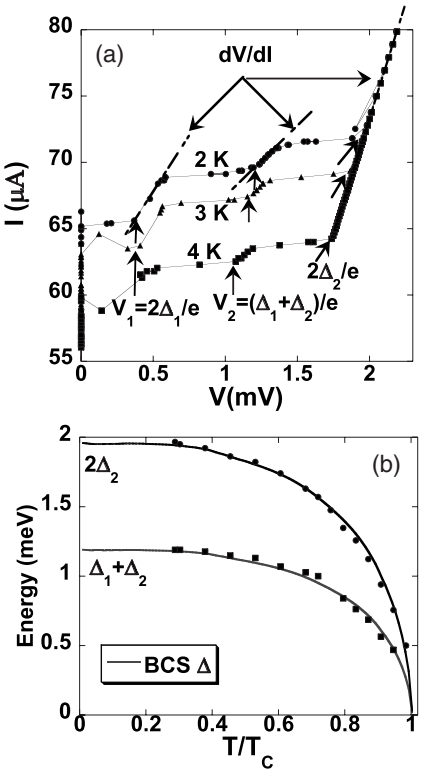

FIG. 4. (a) Current-voltage (I-V) of the $NbSe_2$ NW device. The arrows on each curve indicate, from left to right, voltages corresponding to twice the lower energy gaps ($2\Delta_1$), the sum of the two different gaps ($\Delta_1+\Delta_2$), and twice the high energy gap ($2\Delta_2$). (b) Temperature variations of $2\Delta_2$, and $\Delta_1+\Delta_2$ Solid lines are the fits to the BCS theory.

also reminiscent of Josephson tunnel junctions, where the transition to the linear part of the I-V occurs at a voltage corresponding to twice the energy gap. To further explore the possibility of this scenario, the energy associated with the transition as indicated by arrows denoted as $2\Delta_2/e$ is plotted as a function of temperature in Fig. 4(b). The data fit well to the BCS theory [the top solid line in Fig. 4(b)] for the entire temperature range below a single $T_C(\sim 6.6$ K). From the fit, $\Delta_2(0)$ is determined to be approximately 1.0 meV, yielding $\Delta_2(0)/k_BT_C \approx 1.76$. Therefore, both the temperature dependence and the zero temperature energy of the transition to the linear I-V region are in good agreement with the BCS theory, indicating that the I-V characteristic at finite voltages in our NW is possibly associated with the quasiparticle tunneling of a Josephson junction.

The two mini-current-jumps [indicated by the arrows denoted as V_1 and V_2 in Fig. 4(a)] can be understood in the context of tunneling between two multigap superconducting grains. As shown in Fig. 4 of Ref. 4, the FS of $NbSe_2$ primarily consists of a small Se-derived pancake surface and two Nb-derived concentric cylindrical FS sheets, with the former contributing barely 5% of the total density of states (DOS). Previous experiments suggested that the superconducting energy gap existing on the Se band is much smaller than that on the Nb bands.[9,16] For a Josephson tunnel junction consisting of two identical two-band superconductors,

four tunneling processes are expected: $\Delta_1 \rightarrow \Delta_1$, $\Delta_1 \rightarrow \Delta_2$, $\Delta_2 \rightarrow \Delta_1$, and $\Delta_2 \rightarrow \Delta_2$, where Δ_1 and Δ_2 are the small and large gaps, respectively. As a result, three current jumps are expected to occur sequentially at $2\Delta_1/e$, $(\Delta_1+\Delta_2)/e$, and $2\Delta_2/e$ in the quasiparticle tunneling region as the voltage increases. Since the FS sheets associated with Δ_2 carry most of the DOS, $\Delta_2 \rightarrow \Delta_2$ is the dominant tunneling process. While the minijump at V_1 disappears quickly above $0.5T_C$, the minijump at V_2 survives until near T_C. $eV_2(T)$ follows a BCS behavior with T_C=6.6 K and $eV_2(0) \approx 1.2$ meV, suggesting that the minijump at V_2 originates from the quasiparticle tunneling between the Se band and the Nb band across the junction: $eV_2=\Delta_1+\Delta_2$.[8,9,37,38] Consequently, the size of the small gap can be determined: $\Delta_1(0) \approx 0.2$ meV. This value agrees with the energy of the minijump at V_1 ($2\Delta_1 \approx 0.4$ meV) for T=2 K. Since both $\Delta_2(T)$ and $[\Delta_1(T)+\Delta_2(T)]$ follow the BCS theory and diminish at a nearly identical T_C, $\Delta_1(T)$ should also be BCS-like. In general, the multigap equation yields a non-BCS T dependence. However, for $\mathrm{DOS}(\Delta_1)/\mathrm{DOS}(\Delta_2) \approx 0.05$ as the ratio of DOS and 0.2 as the gap ratio, we found from the multigap equation that both gaps indeed have the BCS T dependence.

Additional support for the tunneling between two two-band superconductors can be found in the comparison between the experimentally determined critical current and the theoretical calculations. The critical current of Josephson junctions was theoretically calculated by Ambegaokar and Baratoff.[14] They established for a symmetrical superconductor-insulator-superconductor (SIS) Josephson junction: $I_C R_N=(\pi/2e)\Delta(T)\tanh[\Delta(T)/2k_BT]$, where R_N is the normal state resistance of the junction, Δ is the energy gap of the superconductor, e is the elementary charge, and k_B is Boltzmann's constant. For asymmetric junctions ($\Delta_1 \neq \Delta_2$), $I_C(0)R_N=\pi\Delta_1(0)\Delta_2(0)/2e[\Delta_1(0)+\Delta_2(0)]$ at T=0 K.[39] At T=0, the critical current for each tunneling process is determined by R_N and $\Delta(0)$, where R_N is calculated from the slope (dV/dI) of the corresponding current jump. The critical current of the dominant tunneling process ($\Delta_2 \rightarrow \Delta_2$) is 56 μA; the critical currents for the other processes are approximately 5.9 μA ($\Delta_1 \rightarrow \Delta_1$) and 5.8 μA ($\Delta_1 \rightarrow \Delta_2$ and $\Delta_2 \rightarrow \Delta_1$ together). Assuming that these four processes are independent and parallel, the total calculated zero temperature critical current (67.7 μA) is consistent with the experimental critical current (67 μA, when it is extrapolated to zero temperature). The linear temperature dependence of the critical current near T_C [Fig. 2(a)] is also in qualitative agreement with the predictions of Ambegaokar and Baratoff.[14] However, the temperature dependence of the critical current in the medium temperature range below T_C deviates from the Ambegaokar and Baratoff relation, which requires further investigations. While the exact origin of the Josephson tunnel junction is unclear, we speculate that the dc Josephson effect may occur at the boundary between two nanoscale crystalline $NbSe_2$ grains. It was found that the critical current of polycrystalline $YBa_2Cu_3O_{7-\delta}$ can be described by assuming formation of grain boundary Josephson junctions.[40] As mentioned earlier, grain boundaries may exist in our NWs.

Although we cannot completely rule out the possibility that the quantitative agreement between our data on a selected $NbSe_2$ NW and the multigap tunneling scenario is merely a coincidence, we believe that this scenario is worth being presented as an alternative explanation of the data on the 75 nm $NbSe_2$ NW and merits further investigations. Finally, we point out that multiple SIS-type grain boundary junctions may exist in an individual $NbSe_2$ NW and the critical current (maximum supercurrent) of each junction is inversely proportional to the R_N of the junction. Therefore, it is the junction with the highest R_N that determines the critical current as well as the quasiparticle tunneling characteristics of the NW. Our 75 nm high quality $NbSe_2$ NW device has relatively high extrapolated zero temperature critical current density (1.5×10^6 A cm^{-2}) and very weak magnetic field dependence (a magnetic field of B=0.3 applied perpendicular to the wire axis only slightly suppresses I_C), which is not unusual for natural grain boundary junctions.[41] The very weak magnetic field modulation of the critical current in our devices can also be attributed to the small sizes of the junctions. Moreover, the magnetic flux penetrates the entire grains across the barrier, leading to significantly reduced magnetic field difference between within the barrier and inside the grains. Unfortunately, the high quality $NbSe_2$ NW was destroyed by electrostatic dissipation before detailed measurements of the magnetic field dependent I-V characteristic could be carried out.

IV. CONCLUSIONS

In conclusion, we have investigated the resistance and V-I characteristics of individual $NbSe_2$ NWs. Overall, the V-I characteristics and critical current density of the NWs can be described by the PSC model. Evidence of TAPS and QPS mechanisms has also been observed in slightly underconverted $NbSe_2$ NWs. A close examination of the temperature dependences of the data on a selected 75 nm NW leads to a possible alternative explanation of the stairlike structure in the V-I characteristic and the critical current. Based on the alternative multigap tunneling junction model, two distinct superconducting gaps are extracted from the I-V characteristic of the 75 nm sample, and both gaps follow the BCS-like temperature dependence vanishing at a common T_C. The extrapolated zero temperature values for the low and high energy gaps (approximately 0.20 and 1.0 meV, respectively) are consistent with previous studies. Although the grain boundary tunnel junction scenario provides a possible explanation of our data obtained from a high quality $NbSe_2$ NW to support the recent theoretical predictions of two distinct energy gaps in $NbSe_2$,[4] further experimental studies are needed to fully understand the nature of the junctions in $NbSe_2$ NWs.

ACKNOWLEDGMENTS

The authors would like to thank Pam Fleming for technical assistance and David Christen, James Thompson, and David Singh for helpful discussions. This research was sponsored by the Division of Materials Sciences and Engineering, Office of Basic Energy Sciences, U.S. Department of Energy, under Contract No. DE-AC05-00OR22725 with Oak Ridge

National Laboratory, managed and operated by UT-Battelle, LLC. Z.X. and P.S. acknowledge the support by the U.S. Department of Energy under Grants Nos. DE-FG02-06ER46334 and DE-FG02-98ER45707, respectively. Part of this research was conducted at the Center for Nanophase Materials Sciences, which is sponsored at Oak Ridge National Laboratory by the Division of Scientific User Facilities, U.S. Department of Energy.

*Author to whom correspondence should be addressed. Present address: Department of Physics and Astronomy, Wayne State University, Detroit, Michigan 48201. zhouz@ornl.gov or zxzhou@wayne.edu

[1] P. Szabó, P. Samuely, J. Kacmarcík, T. Klein, J. Marcus, D. Fruchart, S. Miraglia, C. Marcenat, and A. G. M. Jansen, Phys. Rev. Lett. **87**, 137005 (2001).
[2] M. Iavarone, G. Karapetrov, A. E. Koshelev, W. K. Kwok, G. W. Crabtree, D. G. Hinks, W. N. Kang, E.-M. Choi, H. J. Kim, H.-J. Kim, and S. I. Lee, Phys. Rev. Lett. **89**, 187002 (2002).
[3] R. S. Gonnelli, D. Daghero, G. A. Ummarino, V. A. Stepanov, J. Jun, S. M. Kazakov, and J. Karpinski, Phys. Rev. Lett. **89**, 247004 (2002).
[4] M. D. Johannes, I. I. Mazin, and C. A. Howells, Phys. Rev. B **73**, 205102 (2006).
[5] Z. L. Xiao, O. Dogru, E. Y. Andrei, P. Shuk, and M. Greenblatt, Phys. Rev. Lett. **92**, 227004 (2004).
[6] R. Sooryakumar and M. V. Klein, Phys. Rev. Lett. **45**, 660 (1980).
[7] B. P. Clayman and R. F. Frindt, Solid State Commun. **9**, 1881 (1971).
[8] H. F. Hess, R. B. Robinson, and J. V. Waszczak, Phys. Rev. Lett. **64**, 2711 (1990).
[9] T. Yokoya, T. Kiss, A. Chainani, S. Shin, M. Nohara, and H. Takagi, Science **294**, 2518 (2001).
[10] Y. S. Hor, U. Welp, Y. Ito, Z. L. Xiao, U. Patel, J. F. Mitchell, W. K. Kwok, and G. W. Crabtree, Appl. Phys. Lett. **87**, 142506 (2005).
[11] W. J. Skocpol, M. R. Beasley, and M. Tinkham, J. Low Temp. Phys. **16**, 145 (1974).
[12] D. Y. Vodolazov, F. M. Peeters, L. Piraux, S. Matefi-Tempfli, and S. Michotte, Phys. Rev. Lett. **91**, 157001 (2003).
[13] S. Michotte, S. Matefi-Tempfli, L. Piraux, D. Y. Vodolazov, and F. M. Peeters, Phys. Rev. B **69**, 094512 (2004).
[14] V. Ambegaokar and A. Baratoff, Phys. Rev. Lett. **11**, 104 (1963).
[15] Y. S. Hor, Z. L. Xiao, U. Welp, Y. Ito, J. F. Mitchell, R. E. Cook, W. K. Kwok, and G. W. Crabtree, Nano Lett. **5**, 397 (2005).
[16] R. Corcoran, P. Meeson, Y. Onuki, P.-A. Probst, M. Springford, K. Takita, H. Harima, G. Y. Guo, and B. L. Gyorffy, J. Phys.: Condens. Matter **6**, 4479 (1994).
[17] G. Yi and W. Schwarzacher, Appl. Phys. Lett. **74**, 1746 (1999).
[18] F. Sharifi, A. V. Herzog, and R. C. Dynes, Phys. Rev. Lett. **71**, 428 (1993).
[19] J. A. R. Stiles, D. L. Williams, and M. J. Zuckermann, J. Phys. C **9**, L489 (1976).
[20] C. Berthier, P. Molinie, and D. Jerome, Solid State Commun. **18**, 1393 (1976).
[21] W. Henderson, E. Y. Andrei, M. J. Higgins, and S. Bhattacharya, Phys. Rev. Lett. **77**, 2077 (1996).
[22] M. Danckwerts, A. R. Goñi, and C. Thomsen, Phys. Rev. B **59**, R6624 (1999).
[23] M. R. Eskildsen, M. Kugler, S. Tanaka, J. Jun, S. M. Kazakov, J. Karpinski, and O. Fischer, Phys. Rev. Lett. **89**, 187003 (2002).
[24] T. K. Hunt, Phys. Rev. **151**, 325 (1966).
[25] D. P. Young, M. Moldovan, and P. W. Adams, Phys. Rev. B **70**, 064508 (2004).
[26] L. G. Neumann, Y. D. Dai, and Y. H. Kao, J. Low Temp. Phys. **49**, 457 (1982).
[27] W. J. Skocpol, Phys. Rev. B **14**, 1045 (1976).
[28] A. Falk, M. M. Deshmukh, A. L. Prieto, J. J. Urban, A. Jonas, and H. Park, Phys. Rev. B **75**, 020501(R) (2007).
[29] A. Rogachev and A. Bezryadin, Appl. Phys. Lett. **83**, 512 (2003).
[30] U. Schulz and R. Tidecks, J. Low Temp. Phys. **71**, 151 (1988).
[31] J. Meyer and G. v. Minnigerode, Phys. Lett. **38A**, 529 (1972).
[32] N. Giordano, Phys. Rev. Lett. **61**, 2137 (1988).
[33] N. Giordano, Phys. Rev. B **43**, 160 (1991).
[34] M. Tian, J. Wang, J. S. Kurtz, Y. Liu, M. H. W. Chan, T. S. Mayer, and T. E. Mallouk, Phys. Rev. B **71**, 104521 (2005).
[35] M. Tian, J. Wang, J. Snyder, J. Kurtz, Y. Liu, P. Schiffer, T. E. Mallouk, and M. H. W. Chan, Appl. Phys. Lett. **83**, 1620 (2003).
[36] R. S. Keizer, M. G. Flokstra, J. Aarts, and T. M. Klapwijk, Phys. Rev. Lett. **96**, 147002 (2006).
[37] F. D. Callaghan, M. Laulajainen, C. V. Kaiser, and J. E. Sonier, Phys. Rev. Lett. **95**, 197001 (2005).
[38] E. Boaknin, M. A. Tanatar, J. Paglione, D. Hawthorn, F. Ronning, R. W. Hill, M. Sutherland, L. Taillefer, J. Sonier, S. M. Hayden, and J. W. Brill, Phys. Rev. Lett. **90**, 117003 (2003).
[39] A. G. Sun, D. A. Gajewski, M. B. Maple, and R. C. Dynes, Phys. Rev. Lett. **72**, 2267 (1994).
[40] W. Widder, L. Bauernfeind, H. F. Braun, H. Burkhardt, D. Rainer, M. Bauer, and H. Kinder, Phys. Rev. B **55**, 1254 (1997).
[41] F. Tafuri and J. R. Kirtley, Rep. Prog. Phys. **68**, 2573 (2005).